Electronic Supplementary Information (ESI)

Electronic modulation of single and dual-atom Ru catalysts for the N_2 activation by nanosheet supports

Li Zhao[1], Xiaofan Liu[1], Qiuyue Wang[1], Yanyan Xi[2], Xufeng Lin[1,3*]

[1]College of Chemistry and Chemical Engineering, China University of Petroleum (East China), Qingdao, P.R. China, 266580

[2]Advanced Chemical Engineering and Energy Materials Research Center, China University of Petroleum (East China), Qingdao, P. R. China, 266580

[3]State Key Laboratory of Heavy Oil Processing, China University of Petroleum (East China), Qingdao, P.R. China, 266580

Table of content

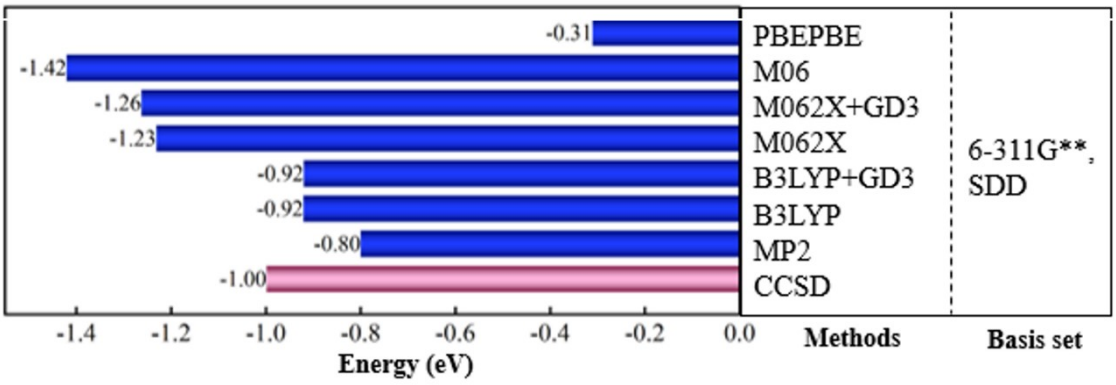

Figure S1. The results of benchmark test for methods and basis sets on the singlet-triplet energy split of $Ru_{SA}H_2$ catalysts.

To identify a suitable theoretical method for N_2 activation on Ru single-atom catalysts (Ru-SACs), we performed a benchmark test on the singlet-triplet energy split of $Ru_{SA}H_2$ (SA denotes single atom), which is a primary activation center employed in this work. We compared the results of seven popular methods—including wavefunction methods (CCSD, MP2) and DFT functionals (B3LYP, M06-2X, PBEPBE, B3PW91) — for calculating intermediates. We also considered the effect of dispersion on the reaction and employed Grimme's D3 dispersion correction, with results shown in Figure S1. Figure S1 shows that B3LYP and B3LYP+GD3 functionals provide the more consitent results with the CCSD or MP2 results than other functionals. Results from B3LYP and B3LYP+GD3 is rather close. Although GD3 may provide accuracy in weak-interaction issues, the interested systems in this work are basically strong-interaction system. Therefore by balancing the computational expense and accuracy for the reaction systems interested in this paper, B3LYP, the busiest “working horse” in DFT functionals was chosen for further study.

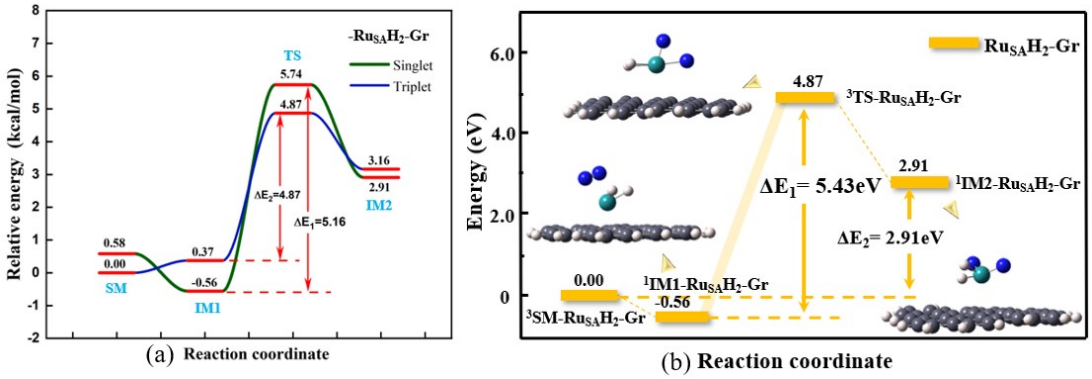

Figure S2. Shown is the energy profiles of N_2 activation on the singlet and triplet Ru-SAC with graphene support on the potential energy surfaces without spin transition, i.e. the **^{1}SM-Ru$_{SA}$H$_2$-Gr → ^{1}IM1-Ru$_{SA}$H$_2$-Gr → ^{1}TS-Ru$_{SA}$H$_2$-Gr → ^{1}IM2-Ru$_{SA}$H$_2$-Gr** and **^{3}SM-Ru$_{SA}$H$_2$-Gr → ^{3}IM1-Ru$_{SA}$H$_2$-Gr → ^{3}TS-Ru$_{SA}$H$_2$-Gr → ^{3}IM2-Ru$_{SA}$H$_2$-Gr** pathways, respectively (a). The energy profiles for the most favorable pathway (MFP) of N_2 activation on Ru-SAC with graphene support, i.e. the **^{3}SM-Ru$_{SA}$H$_2$-Gr → ^{1}IM1-Ru$_{SA}$H$_2$-Gr → ^{3}TS-Ru$_{SA}$H$_2$-Gr → ^{1}IM2-Ru$_{SA}$H$_2$-Gr** pathway (b), which is same as the panel of Figure 5c in the manuscript. See the species notation definition in Section 2.2 in the manuscript as well.

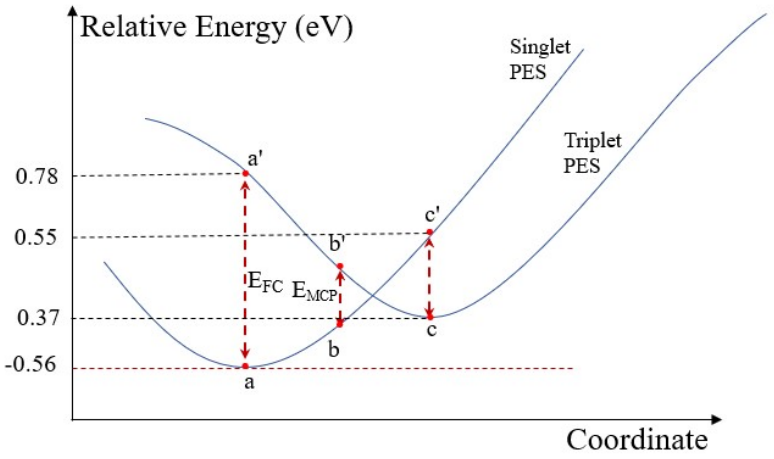

Figure S3. Shown is a simple schematic illustration for the landscape of the energy surface near the energy minimum of singlet and triplet **IM1-$Ru_{SA}H_2$-Gr**. Point a, the energy minimum on the singlet PES, represents the energy of optimized **^{1}IM1-$Ru_{SA}H_2$-Gr**. Point a′ represents the energy of **IM1-$Ru_{SA}H_2$-Gr** in triplet state while having the same geometry as point a. The energy difference of a and a' is the Frank-Condon excitation energy (E_{FC}) at point a. Point b represents the geometry and the energy of **^{1}IM1-$Ru_{SA}H_2$-Gr** where the spin transition occurs with the largest probability. The energy difference of b and b' represents the minimum energy at cross point (MECP). Point c is the energy of optimized **^{3}IM1-$Ru_{SA}H_2$-Gr**. Point c′ represents the energy of **IM1-$Ru_{SA}H_2$-Gr** in singlet state while having the same geometry as point c. The energy difference of c and c' is the E_{FC} at point c, with the geometry of optimized **^{3}IM1-$Ru_{SA}H_2$-Gr**.

Discussion related to Figures S2 and S3.

The relative energy profile for the model graphene sheet (denoted as Gr) supported systems are shown in Figure S2, taking this as an example. Figure 2a shows the energy profiles of N_2 activation on Ru-SAC in singlet and triplet. The energy of the quintet and heptet states is significantly higher than that of the singlet and triplet states, so it is not shown in the Figure S2. For the starting materials (**SM**), the singlet state is higher in energy than the triplet state, which is not surprising since the $Ru_{SA}H_2$ cluster has a triplet ground state. However, it is noteworthy that the first intermediate (**IM1)** has a triplet ground state rather than singlet. In another word, the ground spin state of Ru is changed

during the process of a N_2 molecule approaching a Ru atom. More importantly, both the transition state (**TS**) and the second intermediate (**IM2)** display lower energy on the triplet PES compared to the singlet PES. The activation energy of N_2 activation on Ru-SACs with Gr support, defined as the energy difference between **TS-Ru$_{SA}$H$_2$-Gr** and **IM1-Ru$_{SA}$H$_2$-Gr**, is also lower on the triplet PES (4.87 eV) than on the singlet PES (5.16 eV).

As described in Section 3.2.2 in the manuscript, a spin transition process may lead to alternative reaction pathway when it is rate determining compared to the chemical transformation pathway. In order to show the specific case, Figures S2 and S3 are presented above. The following hypothesis need to be verified, that is, **^{1}IM1-Ru$_{SA}$H$_2$-Gr** is more readily to undergo spin transition to **^{3}IM1-Ru$_{SA}$H$_2$-Gr** which can further proceed to **^{3}TS-Ru$_{SA}$H$_2$-Gr (**the **^{1}IM1-Ru$_{SA}$H$_2$-Gr → ^{3}IM1-Ru$_{SA}$H$_2$-Gr → ^{3}TS-Ru$_{SA}$H$_2$-Gr** pathway), than undergoing an alternative pathway of. **^{1}IM1-Ru$_{SA}$H$_2$-Gr → ^{1}TS-Ru$_{SA}$H$_2$-Gr**. In simple, we define this hypothesis as **Hypothesis A,** i.e., N_2 activation undergoes on the triplet PES.

Based on the energetic data, **Hypothesis A** is valid if **Hypothesis B** is valid, that is, **^{3}IM1-Ru$_{SA}$H$_2$-Gr** can undergo spin transition to ^{1}**IM1-Ru$_{SA}$H$_2$**-Gr with a low spin transition energy (lower than **^{3}IM1-Ru$_{SA}$H$_2$-Gr** going to **^{3}TS-Ru$_{SA}$H$_2$-Gr**). Exact calculation of such spin transition energy, belonging to a "spin-forbidden" process problem [1,2], can be achieved by the "minimum energy at crossing point (MECP)" method. Although in this work we did not calculate the MECP value for the **^{3}IM1-Ru$_{SA}$H$_2$-Gr** species, through two single-point energy calculations (the results shown in Figure S3, see more explanation in its figure caption as well) and logical reasoning Hypothesis B can be verified. Since the energy difference of b→b' is the MECP, which is certainly smaller than a→a' or c→c' ($E_{b\text{-}b'} < E_{a\text{-}a'}$, $E_{b\text{-}b'} < E_{c\text{-}c'}$). From Fig.3, the energy different of points a→a' and c→c' are 1.34 and 0.18 eV, respectively, and thus the energy difference of b→b', or MECP, is lower than 0.18 eV. This comparison consequently verifies that, **^{3}IM1-Ru$_{SA}$H$_2$-Gr** (the same point as c) going to **^{1}IM1-Ru$_{SA}$H$_2$-Gr** (requiring less than 0.18 eV) is much easier than it going to **^{3}TS-Ru$_{SA}$H$_2$-Gr** (requiring 4.87 eV, see Fig.S2a), that is, **Hypothesis B** is verified. Therefore, Hypothesis A is also verified. The verification of **Hypothesis A** mentioned above shows we can use the concept of the most favorable pathway (MFP) to describe the reaction behavior of N_2 activation on SACs, as

shown in Figure S2b or Figure 5c in particular, and Figure 5c-e in general.

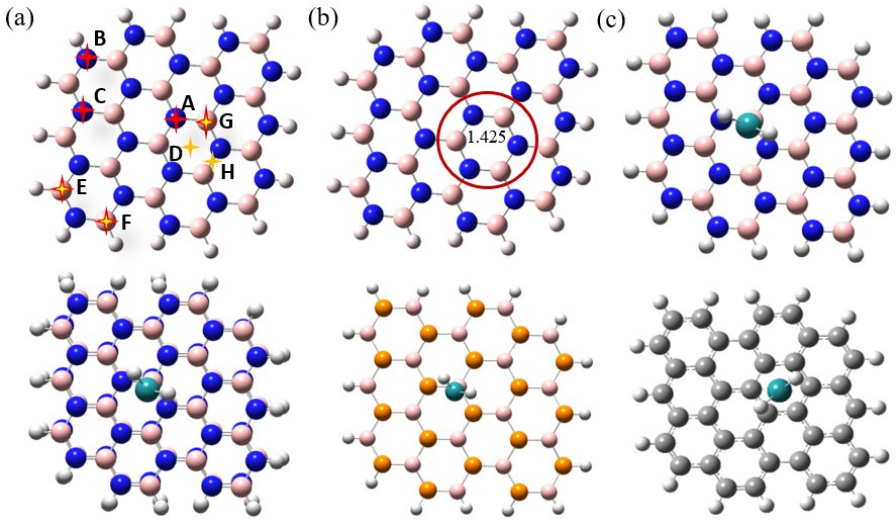

Figure S4. The possible loading positions of a Ru atom on boron nitride nanosheets (a). The optimized structure of monolayer BN nanosheets (b). The most stable structure of Ru single-atom catalysts supported by BN (c), biBN (d), BP (e), Gr (f) nanosheets after optimization.

The possible loading positions of a Ru atom on boron nitride nanosheets is exhibited in Figure S4a. In this paper, we adopt the $B_{19}N_{19}H_{16}$ model as an infinitely extended BN nanosheet model (using BN support as an example, and similarly for other supports). The rationality of this model has been discussed in our previous research and is also explained in Section 2.2 of this paper. Based on this assumption, in this study, the conformations of Ru atoms loaded at positions A, B, and C are consistent, and those loaded at positions E, F, and G are also consistent.

In addition, for all of the structure optimization and energy calculations, all of the atoms were allowed to relax in the red circle, as shown in Figure S4b (This is also explained in section 2.2 in the paper). However, considering that the optimized structure may be related to the designed initial structure, we optimized the initial structures with Ru atoms loaded at positions A, D, H, and G. The results show that the Ru atoms are all adsorbed on B atoms in the optimized structures of these four positions, as shown in Figure S4c.

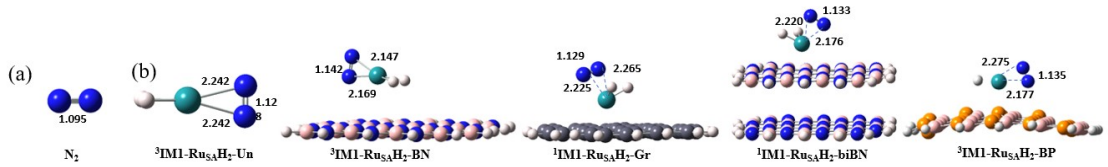

Figure S5. The optimized structures of the N_2 molecule (a) and the first intermediates (IM1, b) formed by N_2 adsorption onto the five catalysts, including the unsupported system (suffix of -Un) and the BN, Gr, BP, and bilayer BN nanosheets (suffix of -biBN) supported system. Key distances are indicated in Å.

Based on the reaction pathway for N_2 activation described in this paper, the adsorption of N_2 on the catalyst surface leads to the formation of the first intermediate (IM1). The optimized structures of IM1 are compiled in Figure S5b. Geometry optimization results indicate that the bond length of free N_2 is 1.095 Å (Figure S5a), which increases to a range of 1.120 - 1.142 Å after adsorption. However, the typical bond length of the N═N double bond is approximately 1.24 Å. This implies that during the N_2 adsorption process, the N≡N triple bond has not yet cleaved into an N═N double bond.

Table S1: The charge of the N atoms and $Ru_{SA}H_2$ cluster in first intermediate for N_2 activation.

	BP	**Gr**	**BN**	**biBN**	**Un**	**N_2 (before adsorption)**
N	-0.046	0.008	-0.099	-0.006	-0.056	**0**
N	-0.063	0.04	-0.093	0.041	-0.056	**0**
2N	-0.109	0.048	-0.192	0.035	-0.112	
$Ru_{SA}H_2$	-0.02	-0.18	0.189	-0.24	0.111	

As shown by the charge results of the Natural population analysis (NPA) presented in Table S1, the N atoms of N_2 molecules within the first intermediate exhibit positive charges, with nearly identical numerical values. This indicates that the two N atoms gain almost the same number of electrons during the adsorption process of N_2 molecules onto both $Ru_{SA}H_2$-Un and $Ru_{SA}H_2$-BN catalysts. For adsorption on $Ru_{SA}H_2$-BP catalysts, there is a notable difference in the number of electrons gained by the two N atoms. When N_2 molecule adsorbed on $Ru_{SA}H_2$-Gr, the two N atoms carry negative charges, meaning they lose electrons—and the extent of electron loss differs significantly between them. As for $Ru_{SA}H_2$-biBN catalysts, the two N atoms lose electrons upon adsorption, with a considerable disparity in the degree of electron loss between the two atoms.

Overall, in the unsupported, BN-, and BP-supported systems, electrons flow from the Ru atom to the N atoms during N_2 adsorption. In contrast, for the Gr- and biBN-supported systems, electron transfer occurs from the N atoms to the Ru atom. These findings demonstrate that the incorporation of different supports significantly modulates the ability of the Ru and N atoms to attract electrons, thereby influencing the adsorption behavior of N_2.

In addition, we speculate that the distance between the Ru atom and the two N atoms in IM1 may be correlated with the extent of charge transfer between them. For instance, in IM1-$Ru_{SA}H_2$-BN, where the two N atoms possess very similar charge values (-0.099 and -0.093), the corresponding Ru…N distances are also quite close (2.169 Å vs. 2.147 Å, the difference is 0.022 Å). Conversely, in IM1-$Ru_{SA}H_2$-biBN, where a significant

difference exists between the charge values on the two N atoms (-0.006 and 0.041), a considerably larger discrepancy is observed between the two Ru…N distances (the difference is 0.044 Å).

References

(1) Harvey, J. N.; Aschi, M. Spin-forbidden dehydrogenation of methoxy cation: a statistical view. *Physical Chemistry Chemical Physics* **1999**, *1* (24), 5555-5563.

(2) Poli, R.; Harvey, J. N. Spin forbidden chemical reactions of transition metal compounds. New ideas and new computational challenges. *Chemical Society Reviews* **2002**, *32* (1), 1-8.